

Scattering of Electromagnetic Waves in Random Media¹

1 Introduction

The problem of wave scattering from a random volume is of interest in many remote sensing problems. For example, a layer of snow above ground constitutes an inhomogeneous medium where the location, shape, size and orientation of ice particles are statistical parameters. Also a forest medium can be considered as a collection of randomly distributed dielectric particles with different geometries, sizes, and dielectrics. As an electromagnetic wave enters such media, wave scattering, attenuation, and depolarization take place. The significance of these phenomena depends on both the physical and electrical properties of the medium as well as the attributes of the incident waves such as the wavelength, incidence angle, and the polarization.

Nowadays advanced high resolution polarimetric and interferometric synthetic aperture radars are used to efficiently gather the radar response of terrestrial targets for wide varieties of remote sensing applications. In order to interpret the remotely sensed data, theoretical models capable of predicting the electromagnetic scattering behavior of random media are needed. Several theoretical approaches are available for interpreting remote sensing measurements. However, it should be noted that because of the complex nature of the scattering problem, exact solutions cannot be found for most practical situations. Therefore, various kinds of simplifications to the physical parameters and approximations to the equations must be applied in order to find a solution. The available models for random media may be categorized into three general groups, semi-empirical models, approximated theoretical models, and numerical/Monte Carlo-based models.

Semi-empirical models consist of simple formulae generated from experimental observations and can be calculated readily [1, 2, 3]. They are often derived heuristically and contain matching parameters that sometimes do not correspond to the physical parameters of the target. Existing theoretical models for electromagnetic backscattering from random media may in turn be categorized into two modeling techniques as well: 1) continuous, and 2) discrete random medium techniques. In the continuous case, the random medium is modeled as an inhomogeneous medium with a random permittivity. Basically, it is assumed that the medium permittivity $\epsilon(x, y, z)$ is a random process whose statistical behavior is known. The analysis of this problem then proceeds in a number

¹Copyright K. Sarabandi, 1997.

of ways. The simplest approach, which is applicable to random media with small permittivity fluctuations, is the iterative Born approximation [4]. Another method used to obtain the scattered fields from a continuous random medium is the radiative transport approach [5]. Here, it is assumed that there is no correlation between fields in different directions of propagation, and therefore, the addition of powers rather than the addition of fields holds. The transport equations are obtained in terms of the statistic of $\epsilon(x, y, z)$ [6]. Study of radiative transfer equations has focused on single and multiple scattering, and to keep the formulation tractable, the particles usually are assumed to be spherical. This leads to the absence of depolarization, whereas for natural particles this non-spherical shape is responsible for the generation of significant depolarization in backscattering direction.

In the discrete case, it is assumed that the particles are sparse in the random medium and single scattering theory is applied to evaluate the backscattered energy [7, 8]. In a coherent approach first the mean field is obtained using Foldy's [9] approximation, which defines an equivalent medium for the scattering region, and then the statistics of the scattered field is found by viewing the scatterer as being embedded in the equivalent medium, and invoking the single scattering theory [10, 11]. To simplify the mathematics involved in this technique, the particles usually are assumed to have simple geometric shapes such as cylinders, disks, or spheres. This technique is referred to, in the literature [12], as the distorted-Born approximation. Radiative Transfer (RT) theory can also be applied to random media composed of discrete scatterers. In this case the extinction and phase function of the random medium, two fundamental quantities of the RT equation, are obtained from the single scattering properties of constituent particles [13, 14, 15] and then the transport equations are solved subject to appropriate boundary conditions.

In what follows we first discuss the iterative Born technique applied to half-space tenuous random medium and then we generalize the solution to a multiplayer random medium. A similar approach is applied to a random medium to derive an expression for the average dyadic Green's function of the medium which is referred to as Dyson's equation for the mean field.

2 Scattering of Electromagnetic Waves from a Tenuous Random Medium

Suppose a half-space medium with a planar interface whose permittivity is denoted $\epsilon_1(x, y, z)$ is illuminated by a plane wave from above. Let us assume that $\epsilon_1(x, y, z)$ is a random process whose statistics are known and $\tilde{\epsilon}_1(x, y, z) = \epsilon_1(x, y, z) - \langle \epsilon_1(x, y, z) \rangle$ which represents the fluctuating part of the permittivity function is relatively small. According to perturbation theory the fields inside the random medium are those of a homogeneous medium with permittivity $\langle \epsilon_1(x, y, z) \rangle$ plus some small fluctuations which basically are scattered fields. As will be shown the solution will be expanded in terms

of a series power in Δ proportional to $\max[\tilde{\epsilon}(x, y, z)]$ with unknown coefficients. Mathematically speaking this series converges if $\frac{\tilde{\epsilon}}{\epsilon_{rc}} < 1$ with a high probability where ϵ_{rc} denotes the radius of convergence of the perturbation solution for the scattering problem. With this statement we are emphasizing that for certain values of $\tilde{\epsilon} > \epsilon_{rc}$ the perturbation solution does not provide accurate results independent of number of terms in the perturbation solution.

Geometry of the scattering problem is shown in Fig. 1 where a monochromatic plane wave is incident upon the medium from the upper half-space. The electric field in each region must satisfy the wave equation. In region 1 the Amper's law may be written as:

$$\nabla \times \bar{H}_1 = -i\omega\epsilon_{1m}\bar{E}_1 - i\omega\tilde{\epsilon}_1\bar{E}_1 \quad (1)$$

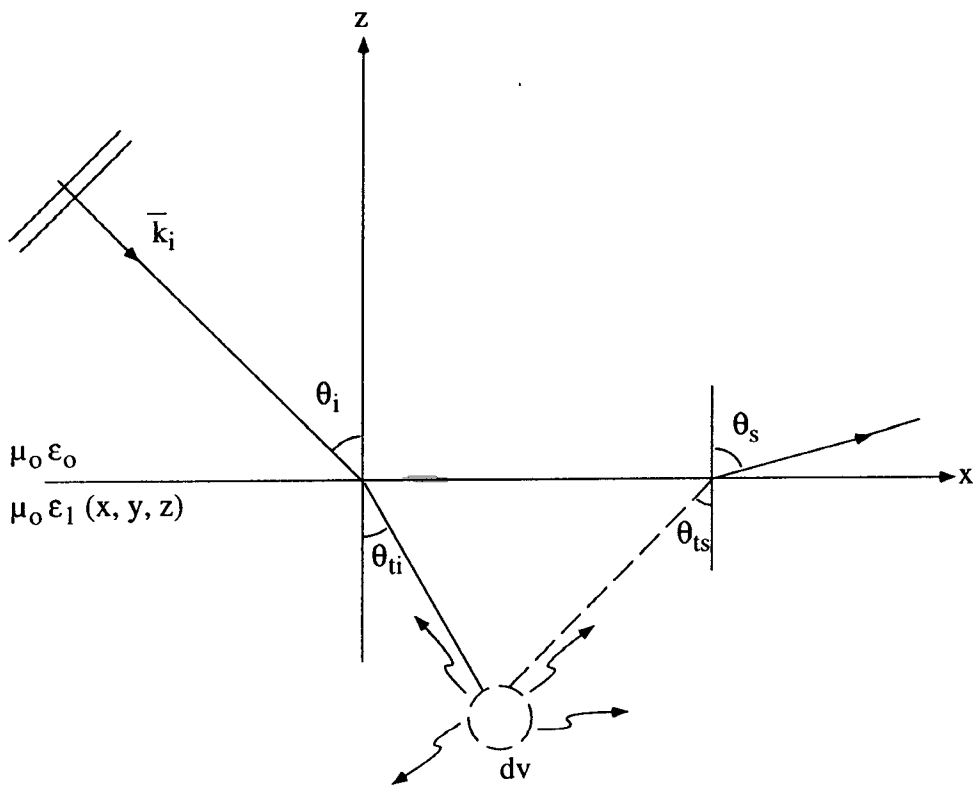


Figure 1: Geometry of plane wave scattering from a tenuous random medium.

where $\epsilon_{1m} = \langle \epsilon_1(x, y, z) \rangle$ and $-i\omega\tilde{\epsilon}_1\bar{E}_1$ may be interpreted as a volumetric current distribution \bar{J}_1 throughout region 1. Hence the wave equation in each region can be written as

$$\nabla \times \nabla \times \bar{E}(\bar{r}) - k_0^2 \bar{E}(\bar{r}) = 0 \quad (\text{no sources}) \quad (2)$$

$$\nabla \times \nabla \times \overline{E}_1(\overline{r}) - k_{1m}^2 \overline{E}_1(\overline{r}) = k_{1f}^2(r) \overline{E}_1(\overline{r}) \quad \text{region 1} \quad (3)$$

In (3) $k_{1f}^2(\overline{r}) = \omega^2 \mu \tilde{\epsilon}_1(\overline{r})$ and $k_{1m}^2 = \omega^2 \mu \epsilon_{1m}$. Let us first assume that the permittivity fluctuation in region 1 approaches zero and region 1 becomes homogeneous. In this case we denote the fields in region 0 and 1 respectively by $\overline{E}^{(0)}(\overline{r})$ and $\overline{E}_1^{(0)}(\overline{r})$ which will be referred to as the zeroth order solutions. Assuming that the incident field is

$$\overline{E}_i(\overline{r}) = [E_{0e} \hat{e}(-k_{zi}) + E_{0h} \hat{h}(-k_{zi})] e^{i\overline{k}_i \cdot \overline{r}} \quad (4)$$

where $\overline{k}_i = k_0(\cos \phi_i \sin \theta_i \hat{x} + \sin \phi_i \sin \theta_i \hat{y} - \cos \theta_i \hat{z})$ and \hat{e} and \hat{h} denote unit vectors along perpendicular and parallel polarizations. The zeroth-order solutions can be obtained easily and are given by

$$\begin{aligned} E^{(0)}(\overline{r}) &= [E_{0e} R_E(\theta_i) \hat{e}(k_{zi}) + E_{0h} R_H(\theta_i) \hat{h}(k_{zi})] e^{i(\overline{k}_{\perp i} + k_{zi} \hat{z}) \cdot \overline{r}} \\ E_1^{(0)}(\overline{r}) &= [E_{0e} \tau_E(\theta_i) \hat{e}(-k_{1zi}) + E_{0h} \tau_H(\theta_i) \hat{h}(-k_{1zi})] e^{i(\overline{k}_{\perp i} - k_{1zi} \hat{z}) \cdot \overline{r}} \end{aligned} \quad (5)$$

where

$$\begin{aligned} R_E(\theta_i) &= \frac{k_{zi} - k_{1zi}}{k_{zi} + k_{1zi}}, \\ R_H(\theta_i) &= \frac{\epsilon_1 k_{zi} - \epsilon_0 k_{1zi}}{\epsilon_1 k_{zi} + \epsilon_0 k_{1zi}}, \\ \tau_E(\theta_i) &= 1 + R_E(\theta_i), \\ \tau_H(\theta_i) &= \frac{k_0}{k_1} (1 + R_H(\theta_i)) \end{aligned} \quad (6)$$

and $k_{1zi} = \sqrt{k_{1m}^2 - k_0^2 \sin^2 \theta_i}$ and $k_{\perp i} = k_0(\cos \phi_i \sin \theta_i \hat{x} + \sin \phi_i \sin \theta_i \hat{y})$. To demonstrate the perturbation equation, let us denote the standard deviation of $k_{1f}^2(\overline{r})$ by Δ , that is,

$$\Delta = \sqrt{\langle k_{1f}^4(\overline{r}) \rangle} = \omega^2 \mu \sqrt{\langle \tilde{\epsilon}^2 \rangle} \quad (7)$$

where Δ is a small quantity. We also define a new random process $f(\overline{r})$ given by

$$k_{1f}^2(\overline{r}) = \Delta f(\overline{r}) \quad (8)$$

For sufficiently small values of Δ , we postulate that the electric field in region 1 can be expanded in terms of a perturbation series given by

$$\overline{E}_1(\overline{r}) = \sum_{n=0}^{\infty} \overline{E}^{(n)}(\overline{r}) \Delta^n \quad (9)$$

Substituting (9) in (3) and collecting the terms of equal power in Δ , it can easily be shown that

$$\nabla \times \nabla \times \overline{E}_1^{(n)}(\overline{r}) - k_{1m}^2 \overline{E}_1^{(n)}(\overline{r}) = f(\overline{r}) E_1^{(n-1)}(\overline{r}) \quad (10)$$

Hence the $(n-1)$ th order solution acts as the source function for the n th order solution. Since the zeroth-order solution exists in principle, the solution to any desired order can be obtained. Denoting the n th order solution in region 0 by $E^{(n)}$ and the Dyadic Green's function of the half-space dielectric by $\overline{\overline{G}}_{ij}(\overline{r}, \overline{r}')$ (i and j denote the region of observation and source points respectively), the n th order scattered fields in each region are given by

$$\overline{E}^{(n)}(\overline{r}) = \int_{-\infty}^0 \int_{-\infty}^0 \int_{-\infty}^{+\infty} \overline{\overline{G}}_{01}(\overline{r}, \overline{r}') \cdot E_1^{(n-1)}(\overline{r}') f(\overline{r}') dx' dy' dz' \quad (11)$$

$$\overline{E}_1^{(n)}(\overline{r}) = \int_{-\infty}^0 \int_{-\infty}^0 \int_{-\infty}^{+\infty} \overline{\overline{G}}_{11}(\overline{r}, \overline{r}') \cdot E_1^{(n-1)}(\overline{r}') f(\overline{r}') dx' dy' dz' \quad (12)$$

since $f(\overline{r})$ is a random process, except for the zeroth-order solution, all higher order scattered fields are random processes as well.

2.1 First-Order Solution

The first-order solution can easily be obtained from the known zeroth-order solution. Usually the interest is in the second moments of the scattered field which can be obtained from

$$\begin{aligned} \langle |\overline{E}^{(1)}(\overline{r})|^2 \rangle &= \int_{\nu} d\overline{r}_1 \int_{\nu} d\overline{r}_2 [\overline{\overline{G}}_{01}(\overline{r}, \overline{r}_1) \cdot \overline{E}_1^{(0)}(\overline{r}_1)] \cdot [\overline{\overline{G}}_{01}(\overline{r}, \overline{r}_2) \cdot \overline{E}_1^{(0)}(\overline{r}_2)]^* \\ &\times \langle f(\overline{r}_1) f^*(\overline{r}_2) \rangle \end{aligned} \quad (13)$$

where $\langle f(\overline{r}_1) f^*(\overline{r}_2) \rangle$ is the two-point correlation function of the normalized permittivity fluctuations. Assuming that the medium is statistically homogeneous, the process becomes stationary, that is,

$$\langle f(\overline{r}_1) f^*(\overline{r}_2) \rangle = C(\overline{r}_1 - \overline{r}_2) \quad (14)$$

Since $C(\overline{r}_1 - \overline{r}_2)$ decays as $|\overline{r}_1 - \overline{r}_2|$ increases, (13) indicates that only adjacent points in the medium contribute to the scattered powers. Therefore, the far-field approximation for the dyadic Green's function may be used in (13). Suppose the observation point

is along $\hat{k}_s = \cos \phi_s \sin \theta_s \hat{x} + \sin \phi_s \sin \theta_s \hat{y} + \cos \theta_s \hat{z}$, then using the stationary phase approximation, the far-field expression for the dyadic Green's function is found to be

$$\bar{G}_{01}(\bar{r}, \bar{r}') \simeq \frac{e^{ikr}}{4\pi r} [\hat{e}(k_{zs}) \hat{e}(k_{1zs}) \tau_E(\theta_s) + \hat{h}(k_{zs}) \hat{h}(k_{1zs}) \tau_H(\theta_s)] e^{-i\bar{k}_{1s} \cdot \bar{r}'} \quad (15)$$

where $\bar{k}_{1s} = k_0 \cos \phi_s \sin \theta_s \hat{x} + k_0 \sin \phi_s \sin \theta_s \hat{y} + k_{1zs} \hat{z}$, and $\tau_E(\theta_s)$ and $\tau_H(\theta_s)$ are Fresnel transmission coefficients from region 1 to region 0. Substituting (15) in (13), we get

$$\langle |E^{(1)}(\bar{r})|^2 \rangle = \frac{1}{16\pi^2 r^2} \left[[\hat{e}(k_{zs}) \hat{e}(k_{1zs}) \tau_E(\theta_s) + \hat{h}(k_{zs}) \hat{h}(k_{1zs}) \tau_H(\theta_s)] \cdot [E_{0e} \tau_E(\theta_i) \hat{e}(-k_{1zs}) + E_{0h} \tau_H(\theta_i) \hat{h}(-k_{1zi})] \right]^2 I \quad (16)$$

where I is given by

$$I = \int_v d\bar{r}_1 \int_v d\bar{r}_2 C(\bar{r}_1 - \bar{r}_2) e^{i[(\bar{k}_{1i} - \bar{k}_{1s}) \cdot \bar{r}_1 + (\bar{k}_{1s}^* - \bar{k}_{1i}^*) \cdot \bar{r}_2]} \quad (17)$$

To evaluate (17) Fourier transform of $C(\bar{r}_1 - \bar{r}_2)$ (normalized power spectral density) can be used. $C(\bar{r}_1 - \bar{r}_2)$ in terms of the power spectral density $W(\beta_x, \beta_y, \beta_z)$ is given by

$$C(\bar{r}_1 - \bar{r}_2) = \frac{1}{(2\pi)^3} \iiint_{-\infty}^{+\infty} W(\bar{\beta}) e^{-i\bar{\beta} \cdot (\bar{r}_1 - \bar{r}_2)} d\bar{\beta} \quad (18)$$

Substituting (18) in (17)

$$I = \frac{1}{(2\pi)^3} \iiint_{-\infty}^{+\infty} d\bar{\beta} W(\bar{\beta}) \int_v d\bar{r}_1 e^{i(\bar{k}_{1i} - \bar{k}_{1s} - \bar{\beta}) \cdot \bar{r}_1} \int_v d\bar{r}_2 e^{-i(\bar{k}_{1i}^* - \bar{k}_{1s}^* - \bar{\beta}) \cdot \bar{r}_2} \quad (19)$$

The first embedded integral can be written as

$$\begin{aligned} \int_{-\infty}^{+\infty} d\bar{r}_{1\perp} e^{i(\bar{k}_{1i\perp} - \bar{k}_{1s\perp} - \bar{\beta}_{\perp}) \cdot \bar{r}_{1\perp}} \int_{-\infty}^0 dz_1 e^{i(-k_{1zi} - k_{1zs} - \beta_z) z_1} = \\ (2\pi)^2 \delta(\bar{k}_{1i\perp} - \bar{k}_{1s\perp} - \bar{\beta}_{\perp}) \frac{i}{\beta_z + k_{1zi} + k_{1zs}} \end{aligned} \quad (20)$$

where the last integral in (20) is evaluated assuming $k_{1zi} + k_{1zs}$ has some positive imaginary part. Noting that the horizontal components of \bar{k}_{1i} and \bar{k}_{1s} are real

$$\bar{k}_{1i\perp}^* - \bar{k}_{1s\perp}^* = \bar{k}_{1i\perp} - \bar{k}_{1s\perp} \quad (21)$$

the integrand of the second embedded integral in (19) evaluated at $\bar{\beta}_\perp = \bar{k}_{1i\perp} - \bar{k}_{1s\perp}$ simplifies to $e^{-i(k_{1iz}^* - k_{1sz}^* - \beta_z)z_2}$ and

$$\begin{aligned} \int_v d\bar{r}_2 e^{-i(\bar{k}_{1i}^* - \bar{k}_{1s}^* - \beta) \cdot \bar{r}_2} \Big|_{\beta_\perp = \bar{k}_{1i\perp} - \bar{k}_{1s\perp}} &= A \int_{-\infty}^0 e^{+i(k_{1iz}^* + k_{1sz}^* + \beta_z)z_2} dz_2 \\ &= A \frac{-i}{\beta_z + k_{1zi}^* + k_{1zs}^*} \end{aligned} \quad (22)$$

where A is the illuminated area. In view of (20) and (22), (19) simplifies to

$$I = \frac{A}{2\pi} \int_{-\infty}^{+\infty} d\beta_z \frac{W(k_{1ix} - k_{1sx}, k_{1iy} - k_{1sy}, \beta_z)}{(\beta_z + k_{1zi}^* + k_{1zs}^*)(\beta_z + k_{1zi}^* + k_{1zs}^*)} \quad (23)$$

The residue theorem can be used to evaluate (23), noting that the power spectral density approaches zero rapidly as β_z approaches infinity. Closing the contour in the upper half-plane (in complex β_z plane) contribution from the pole $\beta_z = -k_{1zi}^* - k_{1zs}^*$ is captured. The power spectral density may also have poles in the upper half-plane, but assuming that $Im[k_{1iz} + k_{1sz}]$ is small the most significant contribution to this integral comes from the pole $\beta_z = -k_{1zi}^* - k_{1zs}^*$. Therefore

$$I \simeq \frac{A}{2} \frac{W(k_{1xi} - k_{1xs}, k_{1yi} - k_{1ys}, -k_{1zi}^* - k_{1zs}^*)}{Im[k_{1zi} + k_{1zs}]} \quad (24)$$

The second moments of the first-order bistatic scattered field may now be evaluated using (16). The four standard components of the bistatic scattering coefficients can be calculated by once transmitting a horizontal polarization ($E_{0h} = 0$) and once a vertical polarization ($E_{0e} = 0$) and then evaluating the vertical and horizontal polarization in each case. Noting that

$$\begin{aligned} \hat{e}(k_{1zs}) \cdot \hat{e}(-k_{1zi}) &= \cos(\phi_s - \phi_i) \\ \hat{e}(k_{1zs}) \cdot \hat{h}(-k_{1zi}) &= \frac{k_{1zi}}{k_{1m}} \sin(\phi_s - \phi_i) \\ \hat{h}(k_{1zs}) \cdot \hat{e}(-k_{1zi}) &= \frac{k_{1zs}}{k_{1m}} \sin(\phi_s - \phi_i) \\ \hat{h}(k_{1zs}) \cdot \hat{h}(-k_{1zi}) &= \frac{1}{k_{1m}^2} [k_{\rho i} k_{\rho s} - k_{1zi} k_{1zs} \cos(\phi_s - \phi_i)] \end{aligned} \quad (25)$$

it can easily be shown that

$$\begin{bmatrix} \sigma_{hh}^\circ(\hat{k}_s, \hat{k}_i) \\ \sigma_{hv}^\circ(\hat{k}_s, \hat{k}_i) \\ \sigma_{vh}^\circ(\hat{k}_s, \hat{k}_i) \\ \sigma_{vv}^\circ(\hat{k}_s, \hat{k}_i) \end{bmatrix} = \frac{\Delta^2 W(k_{1zi} - k_{1xi}, k_{1iy} - k_{1sy}, -k_{1zi}^* - k_{1zs}^*)}{8\pi Im[k_{1iz} + k_{1sz}]} \quad (26)$$

$$\times \begin{bmatrix} |\tau_E(\theta_s)\tau_E(\theta_i)|^2 \cos^2(\phi_s - \phi_i) \\ |\tau_E(\theta_s)\tau_H(\theta_i)|^2 \sin^2(\phi_s - \phi_i) \\ |\tau_H(\theta_s)\tau_E(\theta_i)|^2 \sin^2(\phi_s - \phi_i) \\ |\tau_H(\theta_s)\tau_H(\theta_i)|^2 \left| \frac{1}{k_{1m}^2} [k_{\rho i} k_{\rho s} - k_{1zi} k_{1sz} \cos(\phi_s - \phi_i)] \right|^2 \end{bmatrix}$$

where $k_{\rho i} = k_0 \cos \theta_i$ and $k_{\rho s} = k_0 \cos \theta_s$.

2.2 Second-Order Solution

As demonstrated by equation (12) higher-order scattered fields can be obtained from the previous order solutions. The first-order solution given by (26) does not provide cross-polarized term in backscatter direction ($\phi_s = \phi_i + \pi$). As will be shown in this section the lowest order cross-polarized backscatter appears in the second-order solution. From (11) the second-order scattered field is given by:

$$\bar{E}^{(2)}(\bar{r}) = \int_{-\infty}^0 \int_{-\infty}^{\infty} \bar{G}_{01}(\bar{r}, \bar{r}') \cdot \bar{E}_1^{(1)}(\bar{r}') f(\bar{r}') dx' dy' dz' \quad (27)$$

where $E_1^{(1)}(\bar{r})$, the first-order scattered field in region 1, can be obtained from (12) and is given by:

$$\bar{E}_1^{(1)}(\bar{r}) = \int_{-\infty}^0 \int_{-\infty}^{\infty} \bar{G}_{11}(\bar{r}, \bar{r}') \cdot \bar{E}_1^{(0)}(\bar{r}') f(\bar{r}') dx' dy' dz' \quad (28)$$

Substituting (28) in (27), the second-order scattered field is expressed explicitly

$$\bar{E}^{(2)}(\bar{r}) = \int_v d^3 r_1 \int_v d^3 r_2 \bar{G}_{01}(\bar{r}, \bar{r}_1) \cdot \bar{G}_{11}(\bar{r}_1, \bar{r}_2) \cdot \bar{E}_1^{(0)}(\bar{r}_2) f(\bar{r}_1) f(\bar{r}_2) \quad (29)$$

The scattered power is obtained from

$$\begin{aligned} \langle |\bar{E}^{(2)}(\bar{r})|^2 \rangle &= \int_v \int_v \int_v \int_v d^3 r_1 d^3 r_2 d^3 r_3 d^3 r_4 \left[\bar{G}_{01}(\bar{r}, \bar{r}_1) \bar{G}_{11}(\bar{r}_1, \bar{r}_2) \cdot \bar{E}_1^{(0)}(\bar{r}_2) \right] \cdot \\ &\quad \left[\bar{G}_{01}(\bar{r}, \bar{r}_3) \cdot \bar{G}_{11}(\bar{r}_3, \bar{r}_4) \cdot \bar{E}_1^{(0)}(\bar{r}_4) \right]^* \langle f(\bar{r}_1) f(\bar{r}_2) f(\bar{r}_3) f(\bar{r}_4) \rangle \end{aligned} \quad (30)$$

Since $f(\bar{r})$ is a Gaussian process, $f(\bar{r}_1), \dots, f(\bar{r}_4)$ are jointly Gaussian and it can be shown that

$$\begin{aligned} \langle f(\bar{r}_2)f(\bar{r}_3)f(\bar{r}_4) \rangle &= C(\bar{r}_1 - \bar{r}_2)C(\bar{r}_3 - \bar{r}_4) + C(\bar{r}_1 - \bar{r}_3)C(\bar{r}_2 - \bar{r}_4) \\ &+ C(\bar{r}_1 - \bar{r}_4)C(\bar{r}_2 - \bar{r}_3) \end{aligned} \quad (31)$$

The first term of (31) gives rise to an expression which is equal to the power of the mean second-order scattered field

$$|\langle E^{(2)}(\bar{r}) \rangle|^2 = \left| \int_{\nu} d^3r_1 \int d^3r_2 \bar{\bar{G}}_{01}(\bar{r}, \bar{r}_1) \cdot \bar{\bar{G}}_{11}(\bar{r}_1, \bar{r}_2) \cdot \bar{E}_1^{(0)}(\bar{r}_2) C(\bar{r}_1 - \bar{r}_2) \right|^2 \quad (32)$$

Noting that this term exists only along the specular direction it does not contribute to the backscatter except for the normal incidence. At normal incidence the contribution from this term is negligible compared to the other two terms. Substituting the expression for $E_1^{(0)}(\bar{r})$ (equation5) and the far-field expression for $\bar{\bar{G}}_{01}(\bar{r}, \bar{r}')$ and the integral representation of $\bar{\bar{G}}_{11}(\bar{r}, \bar{r}')$ in (30) expressions for the second-order cross polarized term can be obtained [16].

2.3 Determination of Pair Correlation Function

Apart from the obvious sensor parameters such as incidence and scattering angles as well as the mean permittivity of medium 1, the power spectral density and the extinction coefficient ($2Im[k_{1iz} + k_{1sz}]$) are the most significant parameters influencing the angular behavior and the level of bistatic scattering coefficients. In practice, determination of the pair correlation function, or equivalently the power spectral density, is not straightforward. Noting that the power spectral density must be a positive quantity, the pair correlation function cannot be an arbitrary function. Radially symmetric Gaussian and exponential functions are usually considered as pair correlation functions. The exponential correlation function is appropriate for media where the particles (permittivity discontinuities) are arranged in a completely random fashion in space independent of their size [Debye 1957]. This of course is only an approximation as solid particles cannot overlap. The exponential approximation becomes invalid for media with crystalline or semi-crystalline structures. For these structures it is expected that at a certain distance from a particle there would be no particle with a high probability. This implies a negative value for the correlation function which is not predicted by either Gaussian or exponential pair correlation functions. In practice the correlation function is determined either experimentally or numerically via a Monte Carlo simulation.

In experimental procedures, particle arrangement of the random medium is captured by taking photographs of the slices of the medium which is then digitized and processed to calculate the correlation function. For media such as snow where slices of the medium

cannot be made without destroying the medium property, a polymer at sub-freezing temperatures may be poured to fill the air gaps and then cured. Afterward the snow is allowed to melt, the solid polymer can be sliced for taking the photos[17]. With this procedure the pair correlation function can be estimated in two dimensions (only planar cuts are available). Hence other assumptions such as azimuthal or spherical symmetry must be imposed for estimating $C(\bar{r}_1 - \bar{r}_2)$ from the 2-D samples. The accurate characterization of the three-dimensional correlation function experimentally is very difficult if not impossible. An alternative approach is Monte carlo simulation. Basically, the particle arrangement within a medium is simulated using a packing algorithm faithful to the physical parameters of the medium such as particle size, orientation distribution functions, and particle density. In addition, many 3-D samples of the medium can be generated from which the pair correlation function may be estimated. Figure 2 shows a sample of a two-dimensional packing algorithm [18] and Figures 3 and 4 show the corresponding pair correlation function and its power spectral density. In this example the correlation function was estimated from over 300 packing realizations of the medium with dimensions $0.2 \times 0.2m$. The particles were assumed to be elliptical where the mean value of each axis of the elliptical particles were chosen to be $2mm$ with a standard deviation of $0.4mm$.

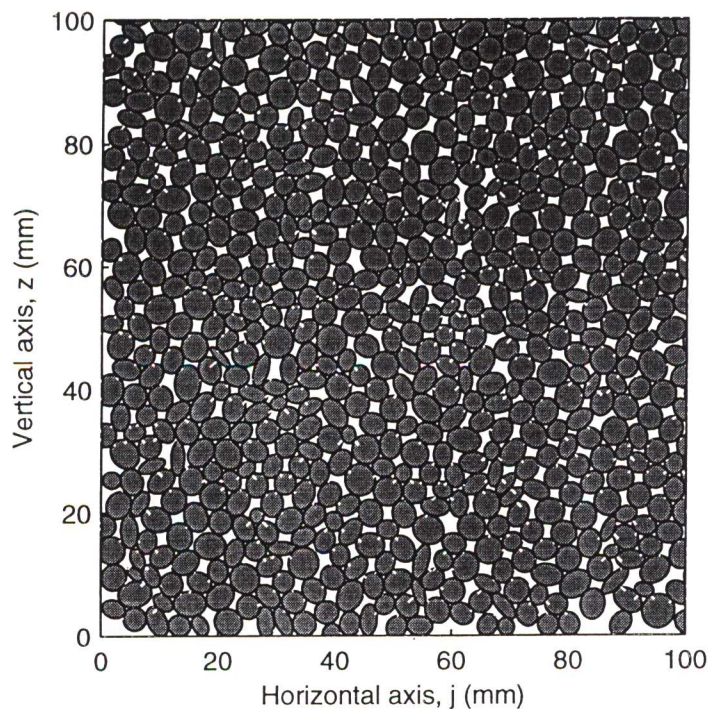


Figure 2: A simulated 2-dimensional random medium with elliptical particles with axes of $2mm \pm 0.4mm$. Volume fraction is 80 % [18].

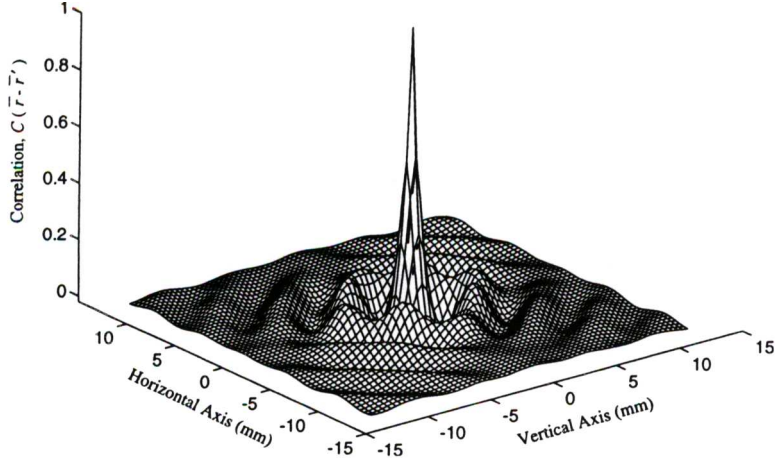


Figure 3: The 2-dimensional correlation coefficient of the medium shown in Fig.2.

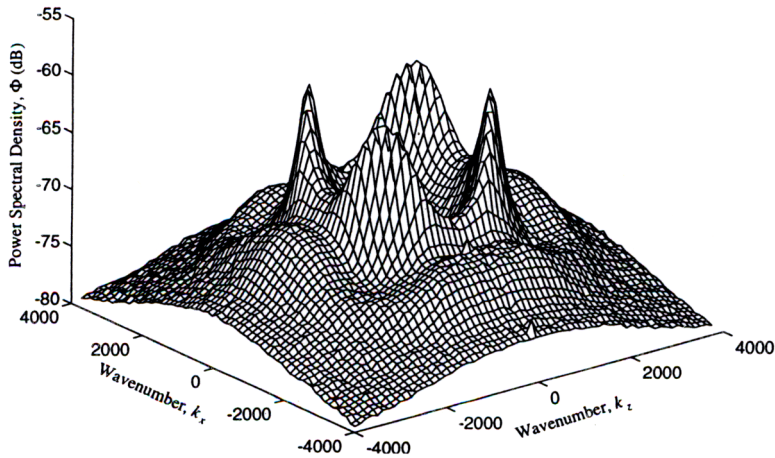


Figure 4: The 2-dimensional power spectral density of the medium shown in Fig.2.

Equation (26) indicates that, depending on the incidence and scattering angles and operating frequency, the bistatic scattering coefficients are probing different points of the power spectral density. Hence errors in the estimation of the correlation function translates directly to errors in the estimation of the backscattering coefficients. It is common to evaluate the autocorrelation function of each sample and then average them to get the function for relatively small values of $|\bar{r} - \bar{r}'|$. Usually the tail of the correlation function so obtained is incorrect. A difficulty may arise from this error in a sense that the Fourier transform of this correlation function may become negative. Since our interest is the power spectral density, it is better to estimated the power spectral density directly. For a continuous process(in root-mean-squared sense) the power spectral density may be obtained directly from

$$W(k_x, k_y, k_z) \simeq \lim_{\substack{x \rightarrow \infty \\ y \rightarrow \infty \\ z \rightarrow \infty}} \left\{ \frac{1}{xyz} \langle |\int_0^x \int_0^y \int_0^z \tilde{\epsilon}(x, y, z) e^{i(k_x x + k_y y + k_z z)} dx dy dz|^2 \rangle \right\} \quad (33)$$

The most commonly used correlation function is the exponential function as mentioned previously. This correlation function is given by

$$C(\bar{r}) = e^{-r/r_0} \quad (34)$$

and its corresponding spectral density is

$$W(k_x, k_y, k_z) = \frac{r_0^3}{\pi^2 (1 + |\bar{k}|^2 r_0^2)^2} \quad (35)$$

For a two-dimensional medium with exponential correlation function ($C(\bar{\rho}) = e^{-\rho/\rho_0}$) the power spectral density is

$$W(k_x, k_y) = \frac{2\pi\rho_0^3}{(1 + |\bar{k}|^2 \rho_0^2)^{3/2}} \quad (36)$$

3 Scattering from a Multi-layer Random Medium

So far the problem of scattering from a semi-infinite random medium is considered. A similar procedure may be followed to obtain the first-order scattered power from a multi-layer random medium. The geometry of the problem is shown in Figure 5. In this configuration there are N layers out of which at least one medium is assumed to have fluctuating permittivity. In general the permittivity of the n th layer may be represented by $\epsilon_n = \langle \epsilon_n \rangle + \tilde{\epsilon}_n(\bar{r})$ where the fluctuating part, $\tilde{\epsilon}_n(\bar{r})$, is relatively small. It is further assumed that the permittivity fluctuations are uncorrelated in two different regions, i.e.,

$$\langle f_m(\bar{r}_1) f_n(\bar{r}_2) \rangle = \delta_{mn} C_m(\bar{r}_1 - \bar{r}_2) \quad (37)$$

where δ_{mn} is the Kronecker delta function. Under these assumptions the first-order scattered power can be written in a manner similar to (13). According to equation (37) addition of powers for the scattered field from each region holds. That is,

$$\langle |E^{(1)}|^2 \rangle = \sum_{n=1}^N \int_{v_n} d^3 r_1 \int_{v_n} d^3 r_2 \left[\bar{G}_{0n}(\bar{r}, \bar{r}_1) \cdot E_n^{(0)}(\bar{r}_1) \right] \cdot \left[\bar{G}_{0n}(r, r_2) \cdot E_n^{(0)}(r_2) \right]^* \quad (38)$$

$$C_n(\bar{r}_1 - \bar{r}_2)$$

The procedure for far field evaluation is as before. We substitute the far-field expression for the dyadic Green's function, the expression for the zeroth order transmitted field in region n and the Fourier transform of $C_n(\bar{r}_1 - \bar{r}_2)$ in (38) to get the first-order scattered field. According to equation (22) of Chapter 2, $\bar{G}_{0n}(\bar{r}, \bar{r}_1)$ can be written as

$$\begin{aligned} \bar{G}_{0n}(\bar{r}, \bar{r}_1) \simeq & \frac{e^{ik_0 r}}{4\pi r} \left\{ \left[\hat{e}(k_{zs})\hat{e}(-k_{nzs})A_n + \hat{h}(k_{zs})\hat{h}(-k_{nzs})C_n \right] e^{i\bar{K}_{ns}\cdot\bar{r}'} \right. \\ & \left. + \left[\hat{e}(k_{zs})\hat{e}(k_{nzs})B_n + \hat{h}(k_{zs})\hat{h}(k_{nzs})D_n \right] e^{-i\bar{k}_{ns}\cdot\bar{r}'} \right\} \end{aligned} \quad (39)$$

where G_{0n} is obtained from $\bar{G}_{0n}(\bar{r}, \bar{r}_2) = \left[\bar{G}_{n0}(\bar{r}', \bar{r}) \right]^t$. The stationary phase approximation is used to find the far-field approximation. As before $\bar{k}_{ns} = k_0 \sin \theta_s \cos \phi_s \hat{x} + k_0 \sin \theta_s \sin \phi_s \hat{y} + k_{nzs} \hat{z}$ with $k_{nzs} = \sqrt{k_n^2 - k_0^2 \sin^2 \theta_s}$. Coefficients A_n, B_n, C_n and D_n may be obtained from the procedure outlines in Chapter 2. Also the zeroth-order field in region n , required in(38), can be expressed by

$$E_n^0(\bar{r}) = \left[E_n^+ e^{ik_{nzi}z} + E_n^- e^{-ik_{nzi}z} \right] e^{i\bar{k}_{\perp i}\cdot\bar{r}_{\perp}} \quad (40)$$

Coefficients of $+z$ and $-z$ traveling waves can be obtained from the propagation matrix formulation.

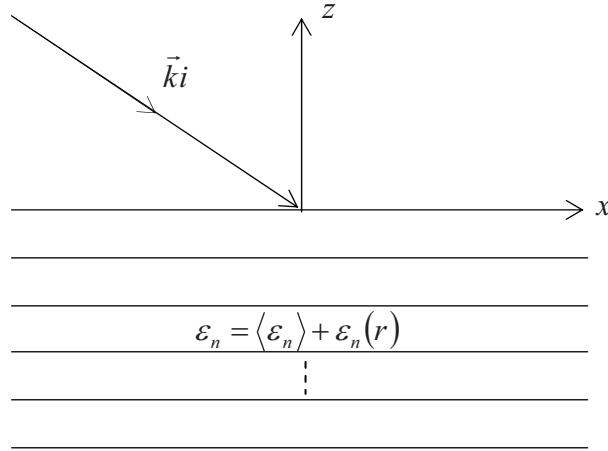


Figure 5: Multi-layer random media illuminated by a plane wave. Layers are statistically independent.

References

- [1] Attema, E. P. W., and F.T. Ulaby, "Vegetation Model as a Water Cloud," *Radio Sci.*, 13, pp. 357-364, 1978.
- [2] Oh, Y., K. Sarabandi, and F. T. Ulaby, "An Empirical Model and an Inversion Technique for radar Scattering from Bare Soil Surfaces," *IEEE Trans. Geosci. Remote Sensing.*, vol. 30, no. 2, 370-381, March 1992.
- [3] Kendra, J. R., and K. Sarabandi, "A Hybrid Experimental/theoretical Scattering Model for Dense random Media," *IEEE Trans. Geosci. Remote Sensing.*, vol. 37, no. 1, pp. 21-35, Jan. 1999.
- [4] Zuniga, M., and J. A. Kong, "Active Remote Sensing of random Media," *J. Appl. Phys.*, vol. 51, pp. 74-79, 1980.
- [5] Ishimaru, A., Wave Propagation and Scattering in Random Media, Vols. 1, 2, New York: Academic, 1978.
- [6] Tsang, L., and J. A. Kong, "Radiative Transfer Theory for Active Remote Sensing of Half-space Random Media," *Radio Sci.*, 13, pp. 763-773, 1978.
- [7] Engheta, N., and C. Elachi, "Radar Scattering from a Diffuse Vegetation Layer Over a Smooth Surface," *IEEE Geoscience and Remote Sensing*, 20, pp. 212-216, 1982.
- [8] Karam, M. A., A. K. Fung, and Y. M. M Antar, "Scattering Models for Vegetation Samples," *Proceedings of IEEE Geoscience and Remote Sensing Symposium*, vol. 2, pp. 1013-1018, 1987.
- [9] Foldy, L. L., "The Multiple Scattering of Waves," *Phys. Rev.*, vol. 67, pp. 107-119, 1945.
- [10] "Discrete Scatter Model for Microwave radar and radiometer response to Corn: Comparison of Theory and Data," *IEEE Trans. Geosci. Remote Sensing*, vol. 32, no. 5, pp. 416-426, March 1994.
- [11] Lin, Y. C., and K. Sarabandi, "A Monte Carlo Coherent Scattering Model for Forest Canopies Using Fractal-Generated Trees," *IEEE Trans. Geosci. Remote Sensing*, vol. 37, no. 1 pp. 440-451, Jan. 1999.
- [12] Rosenbaum, S., and W. Bowles, "Clutter Return from Vegetated Area," *IEEE Trans. Antenna Propag.*, 22, pp. 227-236, 1974.
- [13] Chandrasekhar, S., Radiative Transfer, New York: Dover Publications, 1960.

- [14] Tsang, L., J. A. Kong, and R. T. Shin, Theory of Microwave Remote Sensing, New York: John Wiley and Sons, 1985.
- [15] Sarabandi, K., Electromagnetic Scattering from Vegetation Canopies Ph. D. Thesis, The University of Michigan, 1989.
- [16] Zuniga, M., J. A. Kong, and L. Tsang, "Depolarization Effects in the Active remote Sensing of Random Media," *J. Appl. Phys.*, vol. 51, pp. 2315-2325, 1980.
- [17] Vallese, F., and J. A. Kong, , "Correlation Function Studies for Snow and Ice," *J. Appl. Phys.*, vol 52., pp. 4921-4925, 1981.
- [18] Siqueira, P., K. Sarabandi, and F. T. Ulaby, "Numerical Simulation of Scatterer Positions in a Very Dense Medium with an Application to the Two-Dimensional Born Approximation," *Radio Sci.*, vol. 30, no. 5, pp. Pp1325-1339, 1995.